K. C. Sahu[1]
Department of Chemical Engineering,
Indian Institute of Technology Hyderabad,
Yeddumailaram 502205, Andhra Pradesh, India
e-mail: ksahu@iith.ac.in

O. K. Matar
Department of Chemical Engineering,
Imperial College London,
South Kensington Campus,
London SW7 2AZ, UK
e-mail: o.matar@imperial.ac.uk

Stability of Plane Channel Flow With Viscous Heating

The linear stability analysis of pressure-driven flow undergoing viscous heating through a channel is considered. The walls of the channel are maintained at different constant temperatures and Nahme's law is applied to model the temperature dependence of the fluid viscosity. A modified Orr–Sommerfeld equation coupled with a linearized energy equation is derived and solved using an efficient spectral collocation method. Our results indicate that increasing the influence of viscous heating is destabilizing. It is also shown that the critical Reynolds number decreases by one order of magnitude with increase in the Nahme number. An energy analysis is conducted to understand the underlying physical mechanism of the instability. [DOI: 10.1115/1.4000847]

1 Introduction

The study of flows of viscous fluids with temperature-dependent properties is of great interest in lubrication, tribology, food processing, instrumentation, and viscometry. In the polymer processing industries [1], viscous heating plays an important role as many fluids in such applications strongly depend on temperature because of the coupling between the energy and momentum equations causing profound changes in the flow structure [2–8]. Although a large number of studies have examined the effect of temperature-dependent fluid viscosity and wall heating on flow stability, which have included boundary-layer [9–12], Couette [13–19], channel [20–25], and pipe flows [26,27], viscous heating in Poiseuille channel flow has received far less attention. The main objective of the present paper therefore is to examine the linear stability of pressure-driven channel flow with viscous heating and asymmetrically heated walls.

In literature, the effect of viscous heating has been studied using either Arrhenius-type relationships (see Refs. [16,28]) or a Nahme-type law (see Refs. [15,17–19,29] for instance) to model the temperature-viscosity relationship. Davis et al. [28] and Eldabe et al. [16] used an Arrhenius-type relationship and a Nahme-type law, respectively, to study plane Couette flow and showed that the graph of shear rate against shear stress is monotonic for fluids, which are less sensitive to temperature (as considered in the present study) and S shape for fluids, which are highly sensitive to temperature. The latter also compared the results obtained using both relationships.

The linear stability of channel flow with wall heating was studied by Potter and Graber [20] and Pinarbasi and Liakopoulos [24] who found that the temperature differences between the walls was always destabilizing; this finding was later confirmed by Schäfer and Herwig [21] via an asymptotic analysis of a similar problem. Unlike the above studies, Wall and Wilson [23] and Sameen and Govindarajan [22] rescaled the governing equations using the viscosity of the fluid at the hot wall and the average viscosity across the channel, respectively. Their results, in contradiction to those in Refs. [20,21] indicated that the temperature difference between the walls was stabilizing. Using a transient growth analysis, Sameen and Govindarajan [22] showed that the Prandtl number (taken to be negligible in the linear stability analysis [23]) had a large destabilizing influence. They also studied the effect of buoyancy and found that the Poiseuille–Rayleigh–Bénard mode, which appears at a moderate Grashof number, merged with the Poiseuille mode at high Grashof number. Carrière and Monkewitz [25] showed that the flow was absolutely unstable at very low Reynolds numbers and high Grashof numbers. In all the above studies, the effect of viscous heating, whose study is the main objective of the present paper, was neglected.

The effect of viscous heating in Couette flows was considered by several authors [15,5,17]. They found that the critical Reynolds number decreases as the viscous heating increases. A similar conclusion was also found in Taylor–Couette systems by several authors theoretically [30–33] and experimentally [34,35]. They found that the coupling between the velocity perturbations and the base state temperature gradient is the main mechanism of instability, as it gives rise to spatially inhomogeneous temperature fluctuations, which in turn reduce the local viscosity thereby decreasing the dissipation energy of the disturbances. For very large Pr, Thomas et al. [30] also derived an analytical expression for the critical Reynolds number as a function of the Nahme and Prandtl numbers. Pinarbasi and Imal [29] studied the effect of viscous heating of inelastic fluid flow through a symmetrically heated channel, finding that viscous heating had a destabilizing influence. Of particular interest here is the work of Costa and Macedonio [6], who studied the effect of viscous heating with temperature-dependent viscosity in a symmetrically heated channel flow by linear stability analysis and direct numerical simulations. They found that in certain regimes, viscous heating can trigger and sustain secondary rotational flows. In the present paper, the effect of viscous heating on Poiseuille flow in an *asymmetrically* heated channel is studied, which appears not to have been done previously.

The rest of this paper is organized as follows. The details of the problem formulation are provided in Sec. 2 and the results of the linear stability analysis are presented in Sec. 3. The concluding remarks are provided in Sec. 4.

2 Formulation of the Problem

The pressure-driven, two-dimensional (2D) channel flow of a Newtonian and incompressible fluid with viscous heating is considered, as shown in Fig. 1. The walls are maintained at (different) constant temperatures; $\Delta T \equiv T_u - T_l$, where T_u is the temperature at the top wall. A rectangular coordinate system (x,y) is used to model this flow where x and y denote the horizontal and vertical coordinates. The rigid and impermeable channel walls are located at $y=-H$ and $y=H$. The following Nahme-type viscosity-temperature relationship [36,15,8] is used that approximates the variation in viscosity of many liquids over a wide range of temperature:

[1]Corresponding author.

Contributed by the Fluids Engineering Division of ASME for publication in the JOURNAL OF FLUIDS ENGINEERING. Manuscript received June 1, 2009; final manuscript received December 7, 2009; published online January 12, 2010. Assoc. Editor: Ugo Piomelli.

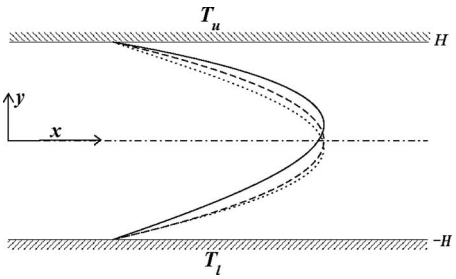

Fig. 1 Schematic diagram of the channel; bottom and top walls are maintained at different, constant temperatures, T_l and T_u, respectively. Also shown here are profiles of the steady, horizontal velocity component generated with Na=0.86, r_T=1 (solid line), Na=0.86, r_T=−0.5 (dotted line), and Na=0, r_T=0 (dashed line).

$$\mu = \mu_l \exp\left[-\frac{\beta(T-T_l)}{T_l}\right] \tag{1}$$

where β is a dimensionless activation energy parameter that stands for the sensitivity of the viscosity to temperature variation; for liquids, β is a positive number and μ_l is the value of the viscosity at T_l.

The following scaling is employed in order to render these equations dimensionless:

$$(x,y) = H(\tilde{x},\tilde{y}), \quad t = \frac{H}{U_m}\tilde{t}, \quad (u,v) = U_m(\tilde{u},\tilde{v}), \quad p = \frac{\mu_l U_m}{H}\tilde{p}$$
$$T = \frac{\tilde{T}T_l}{\beta} + T_l, \quad \mu = \tilde{\mu}\mu_l \tag{2}$$

where u and v denote the horizontal and vertical velocity components and p, ρ, and t denote pressure, density, and time, respectively. The tildes designate dimensionless quantities and U_m is the maximum value of the horizontal velocity component. With the usual Boussinesq approximation, the dimensionless governing equations (after dropping tildes from all nondimensional terms) are then given by

$$\frac{\partial u}{\partial x} + \frac{\partial v}{\partial y} = 0 \tag{3}$$

$$\mathrm{Re}\left[\frac{\partial u}{\partial t} + u\frac{\partial u}{\partial x} + v\frac{\partial u}{\partial y}\right] = -\frac{\partial p}{\partial x} + \left\{\frac{\partial}{\partial x}\left[2\mu\frac{\partial u}{\partial x}\right] + \frac{\partial}{\partial y}\left[\mu\left(\frac{\partial u}{\partial y} + \frac{\partial v}{\partial x}\right)\right]\right\} \tag{4}$$

$$\mathrm{Re}\left[\frac{\partial v}{\partial t} + u\frac{\partial v}{\partial x} + v\frac{\partial v}{\partial y}\right] = -\frac{\partial p}{\partial y} + \left\{\frac{\partial}{\partial x}\left[\mu\left(\frac{\partial u}{\partial y} + \frac{\partial v}{\partial x}\right)\right] + \frac{\partial}{\partial y}\left[2\mu\frac{\partial v}{\partial y}\right]\right\} - \frac{\mathrm{Gr}}{\mathrm{Re}}T \tag{5}$$

$$\mathrm{RePr}\left[\frac{\partial T}{\partial t} + u\frac{\partial T}{\partial x} + v\frac{\partial T}{\partial y}\right] = \mathrm{Na}\mu\left[2\left\{\left(\frac{\partial u}{\partial x}\right)^2 + \left(\frac{\partial v}{\partial y}\right)^2\right\} + \left(\frac{\partial u}{\partial y} + \frac{\partial v}{\partial x}\right)^2\right] + \left[\frac{\partial^2 T}{\partial x^2} + \frac{\partial^2 T}{\partial y^2}\right] \tag{6}$$

where $\mathrm{Re}(\equiv\rho U_m H/\mu_l)$, $\mathrm{Na}(\equiv\beta\mu_l U_m^2/\kappa T_l)$, $\mathrm{Pr}(\equiv c_p\mu_l/\kappa)$, and $\mathrm{Gr}(\equiv\alpha_0 T_l g H^3/\beta\nu^2)$ are the Reynolds, Nahme, Prandtl, and Grashof numbers, respectively; $\nu(\equiv\mu_l/\rho)$ is a kinematic viscosity while κ, c_p, g, and α_0 are coefficient of thermal conductivity, specific heat capacity at constant pressure, the acceleration due to gravity, and the thermal expansion coefficient, respectively. It can be seen that the equations of motion and energy are coupled by the temperature dependence of the viscosity. The extent of coupling increases with Na, which is the product of β and the Brinkman number ($\mathrm{Br}\equiv\mu_l U_m^2/\kappa T_l$).

2.1 Basic State. The base state whose linear stability characteristics will be analyzed, corresponds to a steady, parallel, fully developed flow with vertical thermal stratification.

$$\frac{d}{dy}\left[\mu_0\frac{dU}{dy}\right] = G \tag{7}$$

$$\frac{d^2T_0}{dy^2} + \mathrm{Na}\mu_0\left(\frac{dU}{dy}\right)^2 = 0 \tag{8}$$

where U, G, T_0, and μ_0 represent the horizontal velocity component, constant horizontal pressure gradient, temperature, and viscosity for the basic state. The dimensionless viscosity-temperature relationship for the basic state is given by

$$\mu_0(T_0) = \exp(-T_0) \tag{9}$$

The coupled Eqs. (7) and (8) are solved using a fourth-order Runge–Kutta method and validated against solutions generated using MATLAB with the following boundary conditions:

$$U = 0 \quad \text{at} \quad y = \pm 1 \tag{10}$$

$$T_0 = 0 \quad \text{at} \quad y = -1 \quad \text{and} \quad T_0 = r_T \quad \text{at} \quad y = 1 \tag{11}$$

where $r_T = \beta\Delta T/T_l$.

The basic state velocity profiles obtained above for a constant pressure gradient are then rescaled by the maximum horizontal velocity U_m. Typical basic state profiles of the second derivative of the horizontal velocity component (U'') and temperature (T_0) for different Na when r_T=1 and r_T=−0.5 are shown in Figs. 2(*a*)–2(*d*), respectively. An inspection of Figs. 2(*a*) and 2(*c*) reveals that the tendency of the profiles to become inflectional (U''=0 for a value of y in the channel) increases with Na; the profile is inflectional for Na>0.8 approximately indicating that the flow in inviscidly unstable [37] for these parameter values. These features also indicate that increasing Na is expected to exert a destabilizing influence on the flow. As expected, it can be seen that the inflectional point always lies near the cold wall.

2.2 Linear Stability Analysis. We examine the temporal linear stability of the base state obtained by solving Eqs. (7) and (8) to infinitesimal, 2D disturbances using a normal modes analysis by expressing each flow variable as the sum of a base state and a 2D perturbation [38,39],

$$(u,v,p,T,\mu)(x,y,t) = [U(y),0,P(y),T_0(y),\mu_0(y)] + \mathrm{Real}\{(\hat{u},\hat{v},\hat{p},\hat{T},\hat{\mu})(y)\exp(\iota[\alpha x - \omega t])\}, \tag{12}$$

where the hat decoration designates the perturbation quantities. In Eq. (12), $\hat{\mu} = (d\mu_0/dT_0)\hat{T}$ represents the perturbation viscosity, α is the disturbance wavenumber (real), and ω is a complex frequency. The amplitude of the velocity disturbances are then re-expressed in terms of a streamfunction: $(\hat{u},\hat{v}) = (\psi', -\iota\alpha\psi)$, where the prime denotes differentiation with respect to y. The substitution of Eq. (12) into Eqs. (3)–(6) followed by subtraction of the base state equations, subsequent linearization, and elimination of the pressure perturbation yields the following coupled ordinary differential eigenvalue equations (following the suppression of the hat decoration):

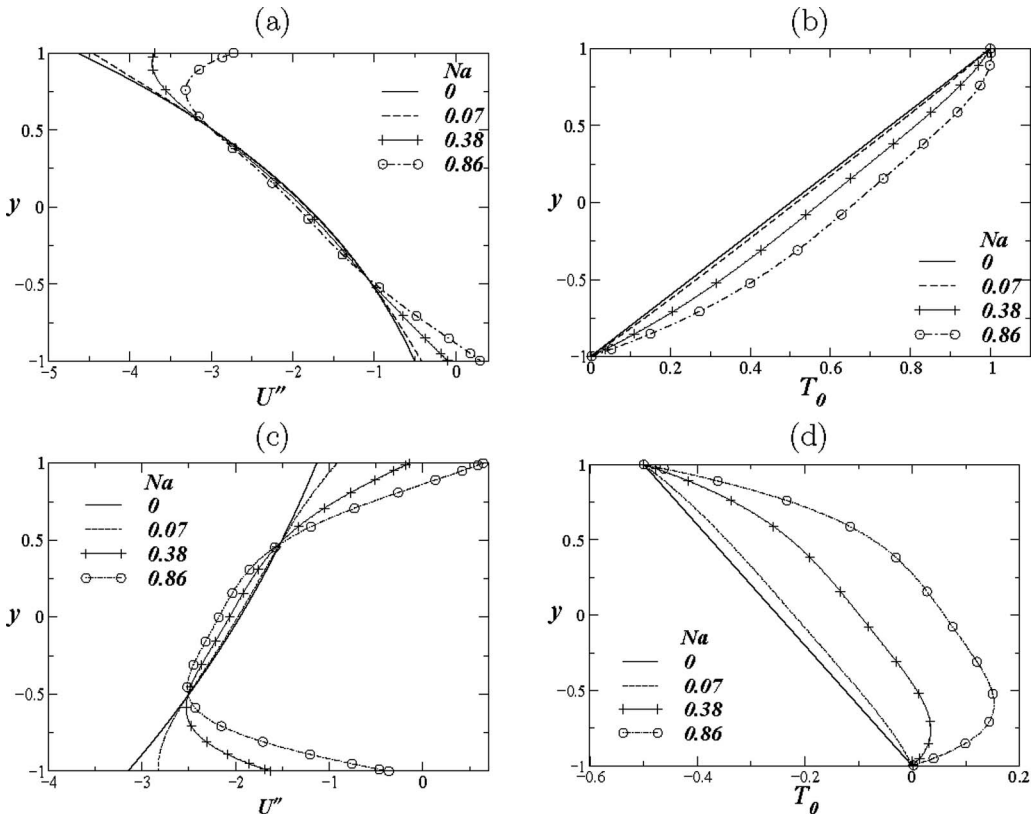

Fig. 2 Basic state profiles of the second derivative of the horizontal component of the velocity (U'') and temperature (T_0) for different Na when $r_T=1$ and $r_T=-0.5$ are shown in (*a*) and (*b*) and (*c*) and (*d*), respectively

$$\iota\alpha[(\psi''-\alpha^2\psi)(U-c)-\psi U'']$$
$$=\frac{1}{\mathrm{Re}}\left[\mu_0(\psi''''-2\alpha^2\psi''+\alpha^4\psi)+2\frac{d\mu_0}{dT_0}T_0'(\psi'''-\alpha^2\psi')\right.$$
$$+\frac{d\mu_0}{dT_0}T_0''(\psi''+\alpha^2\psi)+\frac{d^2\mu_0}{dT_0^2}(T_0')^2(\psi''+\alpha^2\psi)+\frac{d\mu_0}{dT_0}(U'T''$$
$$\left.+2U''T'+\alpha^2U'T+U'''T)+2\frac{d^2\mu_0}{dT_0^2}T_0'U'T'+\frac{d^2\mu_0}{dT_0^2}T_0''U'T\right.$$
$$\left.+\frac{d^3\mu_0}{dT_0^3}(T_0')^2U'T+2\frac{d^2\mu_0}{dT_0^2}T_0'U''T\right]+\frac{\mathrm{Gr}}{\mathrm{Re}^2}\iota\alpha T \tag{13}$$

$$\iota\alpha[(U-c)T-\psi T_0']=\frac{1}{\mathrm{RePr}}[T''-\alpha^2T]+\frac{\mathrm{Na}}{\mathrm{RePr}}2U'\mu_0(\psi''+\alpha^2\psi) \tag{14}$$

where $c(\equiv\omega/\alpha)$ is a complex phase speed of the disturbance. Note that a given mode is unstable if $\omega_i>0$, stable if $\omega_i<0$, and neutrally stable if $\omega_i=0$. The minimum Reynolds number in the neutral stability curve (contour of $c_i=0$ in α against Re plot) is referred to here as a "critical" Reynolds number $\mathrm{Re}_{\mathrm{cr}}$. In the limit $(\mathrm{Na}\to 0)$, these equations reduce to those of Sameen and Govindarajan [22]; and in the limit $(\mathrm{Na},\mathrm{Gr})\to 0$, we obtained the stability equations of Wall and Wilson [23]. We can also recover the Orr–Sommerfeld equation for the special case of $T=0$ and $\mu_0=1$.

The eigenvalue c and the eigenfunctions ψ and T are obtained via the solution of Eqs. (13) and (14) using the Chebyshev spectral collocation method [40], accomplished by the specification of the collocation points chosen to be the Chebyshev Gauss–Lobatto points defined as $y_k=\cos(k\pi/N)$, where $k=(1,N)$ subject to the following boundary conditions:

$$\psi=\psi'=T=0 \quad \text{at } y=\pm 1 \tag{15}$$

where N is the order of Chebyshev polynomials.

The eigenvalue problem is then recast into the following matrix form:

$$\begin{bmatrix}\mathcal{A}_{11} & \mathcal{A}_{12}\\ \mathcal{A}_{21} & \mathcal{A}_{22}\end{bmatrix}\begin{bmatrix}\psi\\ T\end{bmatrix}=c\begin{bmatrix}\mathcal{B}_{11} & \mathcal{B}_{12}\\ \mathcal{B}_{21} & \mathcal{B}_{22}\end{bmatrix}\begin{bmatrix}\psi\\ T\end{bmatrix} \tag{16}$$

and solved using the public domain software LAPACK. A similar technique has previously been used to study the stability of flow through a diverging pipe [40] and interfacial stability of non-Newtonian fluid flow through a channel [39]. The results obtained from the above linear stability analysis are discussed below.

3 Results and Discussion

We begin the presentation of our results by demonstrating their convergence the on refinement of the spatial-mesh. Evidence of this is provided in Fig. 3 in which we plot the neutral stability curves for $r_T=1$, Pr=1, Gr=100, and Na=0.86. The parameter values chosen are characteristic of a situation when the top channel wall is maintained at a higher temperature than that of the bottom wall, with some typical values of Prandtl and Grashof numbers. In this case, one would expect the flow to be more unstable than isothermal channel (e.g., Refs. [22,23]). It can be seen that the curves are indistinguishable for different values of the order of Chebyshev polynomials N. Thus, $N=121$ is used to generate the rest of the stability results in this paper. The neutral stability curve for $r_T=0$, Gr=0, and Na=0, which corresponds to the isothermal flow through a channel, is shown by a dotted line.

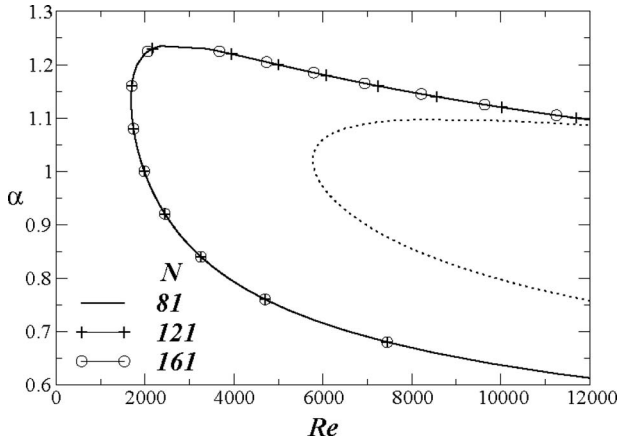

Fig. 3 The effect of increasing the order of Chebyshev polynomials (*N*) on the neutral stability curve with r_T=1, Pr=1, Gr=100, and Na=0.86. The dotted line shows the neutral stability curve for r_T=0, Gr=0, and Na=0, which corresponds to isothermal flow through a channel; the critical Reynolds number for this case is 5772.2.

It can be seen that the critical Reynolds number obtained for this case is 5772.2, which is the same as that of isothermal channel flow [41]. This inspires further confidence in the predictions of our numerical procedure.

In Fig. 4, we investigate the effect of varying r_T, which is equivalent to increasing the temperature difference between the channel walls in the absence of viscous heating and gravity. An inspection of Fig. 4(*a*) reveals that an increase in r_T destabilizes the flow. This observation is the same as that of Ref. [20] and opposite to the finding in Refs. [22,23]. However, this difference is due to the fact that unlike the present study, the authors in Refs. [22,23] used the viscosity at the hot wall (μ_{hot}) as the reference viscosity while scaling the governing equations. It can be seen in Fig. 4(*b*) that the present results agree with those of the latter studies, when we redefine the Reynolds number based on μ_{hot}, $Re_H=\rho U_m H/\mu_{hot}$. Since viscosity of liquid decreases with increasing temperature, the location of the maximum velocity is shifted toward the hot wall, as can also be seen in Fig. 1. This makes the profile less (more) inflectional ($U''=0$) near the hot (cold) wall. It can also be seen in Fig. 4(*b*) that the neutral stability curves for r_T=0.5 and −0.5 are indistinguishable when the Reynolds number is defined based on μ_{hot}, Re_H. This result indicates that the neutral stability curves are symmetrical in r_T for this set of parameters, however, we will see below that this is not true for nonzero Na.

In the rest of this paper, we concentrate on studying the effects of the Nahme number. In Figs. 5(*a*) and 5(*b*), we plot numerically generated dispersion curves (ω_i against α curves) for different values of Na with r_T=1 and r_T=−0.5, respectively. The rest of the parameter values are $Re=10^4$, Pr=1, and Gr=100. The dispersion curves for the symmetrically heated channel (r_T=0, Na=0.86)

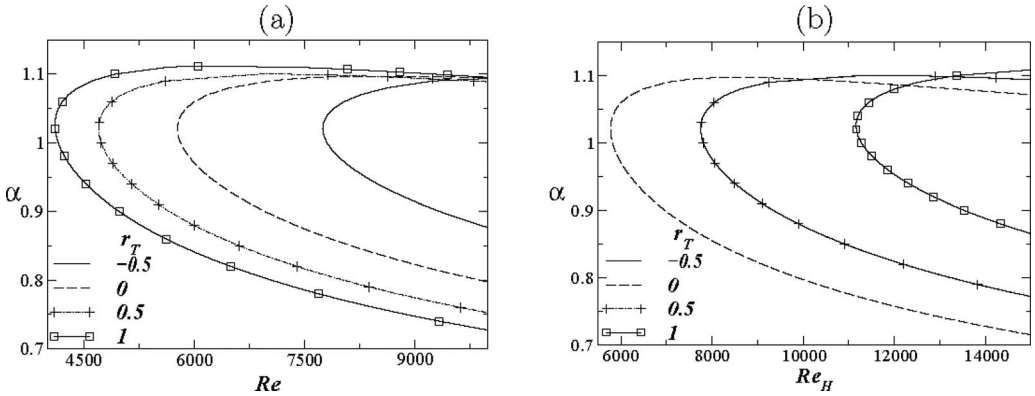

Fig. 4 Stability boundaries for different values of r_T. The rest of the parameter values are Pr=0, Gr=0, and Na=0. In Fig. 4(*b*), $Re_H \equiv U_m \rho H/\mu_{hot}$. Note that the curves associated with r_T=−0.5 and r_T=0.5 in panel (b) are indistinguishable.

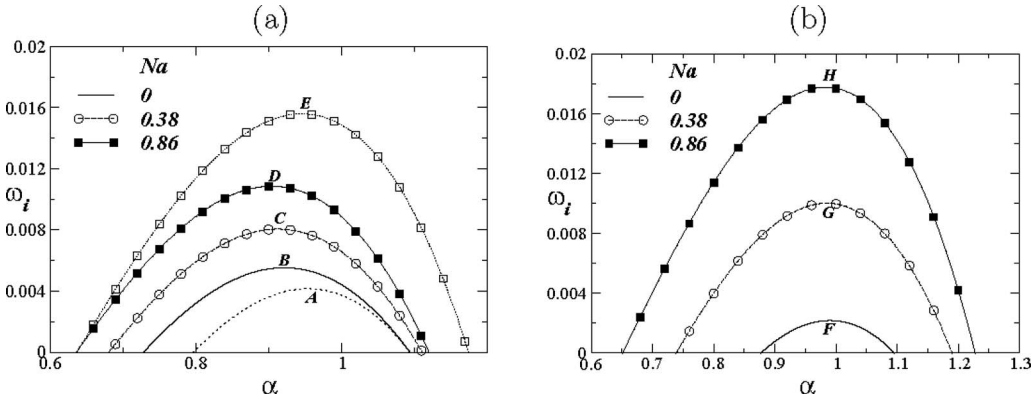

Fig. 5 The effect of varying the Na on the dispersion curves for r_T=1 (*a*) and r_T=−0.5 (*b*). The rest of the parameter values are $Re=10^4$, Pr=1, and Gr=100. The dotted line and the line with the open squares represent the dispersion curves for isothermal channel (r_T=0, Na=0) and symmetrically heated channel flow (r_T=0, Na=0.86). The labels A–E and F–H are used to designate the maxima in the dispersion curves in (*a*) and (*b*), respectively; the energy budgets associated with the points labeled A–E and F–H are provided in Tables 1 and 2, respectively.

Table 1 Energy budgets for the points labeled A–E in Fig. 5(*a*)

Point	REY/KIN	DIS/KIN
A	0.0193	0.0110
B	0.0197	0.0082
C	0.0243	0.0078
D	0.0295	0.0074
E	0.0410	0.0100

Table 2 Energy budgets for the points labeled F–H in Fig. 5(*b*)

Point	REY/KIN	DIS/KIN
F	0.0168	0.013
G	0.0319	0.0124
H	0.0468	0.0117

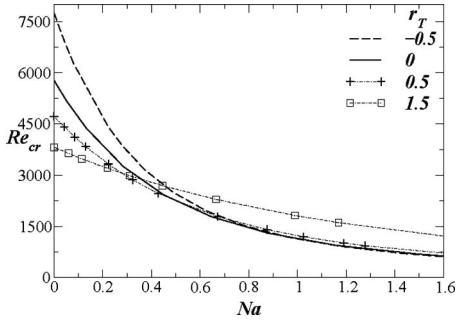

Fig. 6 Variation in the critical Reynolds number with Na for different values of r_T. The rest of the parameter values are Pr =1 and Gr=100.

and isothermal channel ($r_T=0$, Na=0) are also shown in Fig. 5(*a*). The dispersion curves depicted in Fig. 5 are paraboloidal, and $\omega_i>0$ over a finite band of wavenumbers, indicating the presence of a linear instability. It can be seen in Figs. 5(*a*) and 5(*b*) that increasing Na is destabilizing, leading to an increase in the maximal growth rate and to a wider range of wavenumbers over which the flow is unstable for both $r_T=1$ and $r_T=-0.5$. An inspection of Fig. 5(*a*) also reveals that in the presence of viscous heating, the flow through a symmetrically heated (isothermal) channel is more (less) unstable than that of the corresponding asymmetrically heated channel.

In order to gain further insight into the mechanisms underlying the instabilities discussed in the foregoing, we have carried out an analysis of the "energy budget" [38,42] (see Appendix for details). A similar analysis was also performed recently by Sahu and coworkers [39,43] and Sevlam et al. [44] for immiscible non-Newtonian, miscible channel flows and miscible core annular flows, respectively. The energy "budgets" associated with points A–E and F–H, which correspond to the most dangerous modes of the dispersion curves in Figs. 5(*a*) and 5(*b*) are given in Tables 1 and 2, respectively. An inspection of Tables 1 and 2 reveals that the contribution arising from the spatially averaged "Reynolds stress" term, *REY* (viscous dissipation term, *DIS*) increases (decreases) with increase in Na, which makes the flow more unstable. A similar mechanism of instability was found earlier by several authors [30–32] in Taylor–Couette systems. It can also be seen in Table 1 that the contribution arising from the spatially averaged REY (DIS) associated with point A is lower (higher) than that associated with point B, indicating that isothermal channel flow is less unstable than that in an asymmetrically heated channel. A similar comparison of the "energies" associated with points D and E reveals that flow in a symmetrically heated channel is more unstable than that in an asymmetrically heated channel when Na =0.86.

Finally, in Fig. 6 we investigate the variation in critical Reynolds number, defined as the value of Re at which $\omega_i=0$ with Na for different values of r_T. It can be seen that Na is destabilizing for all positive values of r_T investigated in the present work; the "isothermal" critical Reynolds number decreases by an order of magnitude with increasing Na. An inspection of Fig. 6 also reveals that r_T is destabilizing for Na smaller than a critical value Na_c (that depends on the rest of the parameters) but stabilizing above this value. To understand the physical mechanism of this behavior, we plot the dispersion curves for Na=0.1 and 1.1 and $\mathrm{Re}=10^4$ in Figs. 7(*a*) and 7(*b*), respectively. The rest of the parameter values are the same as those used to generate Fig. 6. It can be seen in Figs. 7(*a*) and 7(*b*) that increasing r_T is destabilizing for Na=0.1 and stabilizing for Na=1.1. We also found (not shown) that with the increase in r_T, the Reynolds stress reduces near the cold wall and increases near the hot wall indicating that production near the hot wall is more important than that of the cold wall for the instability; dissipation, however, is almost identical in all the cases.

The destabilizing characteristics of r_T for Na=0.1 can be explained by inspection of the energy budgets of the points labeled A–D, associated with the most dangerous mode in Fig. 7(*a*), which are listed in Table 3. An inspection of Table 3 indicates that the magnitude of the spatially averaged energy dissipation, DIS, decreases with increasing r_T in contrast to that of REY, which remains approximately constant for the range of r_T considered. Similarly, inspection of the energy budgets of the points labeled E–H, associated with the most dangerous mode in Fig. 7(*b*),

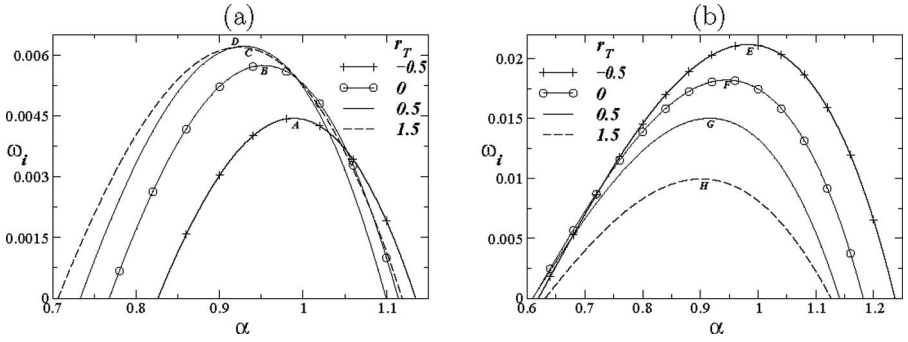

Fig. 7 The effect of varying r_T on the dispersion curves for Na=0.1 (*a*) and Na=1.1 (*b*). The rest of the parameter values are same as those used to generate Fig. 6. The labels A–H are used to designate the maxima in the dispersion curves; the energy budgets associated with these points are provided in Tables 3 and 4.

Table 3 Energy budgets for the points labeled A–D in Fig. 7(*a*)

Point	REY/KIN	DIS/KIN
A	0.0211	0.0128
B	0.0222	0.0108
C	0.022	0.0094
D	0.02	0.0071

Table 4 Energy budgets for the points labeled E–H in Fig. 7(*b*)

Point	REY/KIN	DIS/KIN
E	0.0529	0.011
F	0.0459	0.0095
G	0.0385	0.0083
H	0.026	0.0078

which are listed in Table 4, reveals that REY decreases with increasing r_T. The spatially averaged DIS also decreases but with a slower rate.

4 Conclusions

We have investigated the effect of viscous heating parameterized by a suitably defined Nahme number, Na, on the linear stability of a pressure-driven channel flow with a temperature-dependent viscosity; both symmetrically and asymmetrically heated channel walls are considered. The viscosity-temperature dependence is modeled by a Nahme-type relationship. The modified Orr–Sommerfeld equation for the disturbance streamfunction coupled to a linearized energy equation is derived and solved using a spectral collocation method. Our results indicate that increasing the value of Na, which increases the relative significance of viscous heating, promotes instability. We have also found that increasing r_T, which corresponds to an increase in the temperature difference between the two walls, is more (less) destabilizing for low (high) values of Na.

Acknowledgment

The authors acknowledge the fruitful discussions with Professor Rama Govindarajan. K.S. thanks Uttam Doraswami, Francesco Coletti, and Lennon Ó Náraigh of Imperial College London for their help and encouragement. We also thank the EPSRC for their support through Grant Nos. EP/E046029/1 and EP/D503051 and the DTI through Grant No. TP//ZEE/6/1/21191.

Appendix: Energy Balance

Here we have carried out an energy budget analysis as given in Refs. [38,42]. A similar analysis was also performed recently by Sahu and co-workers [39,43] and Sevlam et al. [44] for immiscible non-Newtonian, miscible channel flows, and miscible core annular flows, respectively. The energy equation is derived by taking the inner product of the horizontal and vertical components of the Navier–Stokes equations with their respective velocity components. The resultant equation is then averaged over the wavelength $2\pi/\alpha$ and integrated over the height of channel.

$$2\omega_i(\mathrm{KIN}) = \mathrm{REY\text{-}DIS} \tag{A1}$$

where

$$\mathrm{KIN} = \int_{-1}^{1} \frac{1}{4}(uu^* + vv^*)dy \tag{A2}$$

$$\mathrm{REY} = -\int_{-1}^{1} \frac{1}{4}U'(uv^* + u^*v)dy \tag{A3}$$

$$\mathrm{DIS} = \int_{-1}^{1} \frac{\mu_0}{\mathrm{Re}}\left[\alpha^2 uu^* + \frac{1}{2}(u' + \iota\alpha v)(u^{*\prime} - \iota\alpha v^*) + v'v^{*\prime}\right]dy \tag{A4}$$

where the superscript * denotes complex conjugate, KIN represents the spatially averaged disturbance kinetic energy, REY denotes the spatially averaged Reynolds stress term, which determines the rate of production of energy due to transfer of energy from the base flow to the disturbances, and DIS corresponds to the spatially averaged viscous dissipation of energy. The above equation allows one to isolate the mechanisms by which energy is transferred from the base flow to the disturbances.

References

[1] Pearson, J. R. A., 1985, *Mechanics of Polymer Processing*, Elsevier, London.
[2] Pearson, J. R. A., 1977, "Variable-Viscosity Flows in Channels With High Heat Generation," J. Fluid Mech., **83**, pp. 191–206.
[3] Ockendon, H., 1979, "Channel Flow With Temperature-Dependent Viscosity and Internal Viscous Dissipation," J. Fluid Mech., **93**, pp. 737–746.
[4] Ockendon, H., and Ockendon, J., 1977, "Variable-Viscosity Flows in Heated and Cooled Channels," J. Fluid Mech., **83**, pp. 177–190.
[5] Wylie, J. J., and Huang, H., 2007, "Extensional Flows With Viscous Heating," J. Fluid Mech., **571**, pp. 359–370.
[6] Costa, A., and Macedonio, G., 2005, "Viscous Heating Effects in Fluids With Temperature-Dependent Viscosity: Triggering of Secondary Flows," J. Fluid Mech., **540**, pp. 21–38.
[7] Pinarbasi, A., and Ozalp, C., 2005, "Influence of Variable Thermal Conductivity and Viscosity for Nonisothermal Fluid Flow," Phys. Fluids, **17**, p. 038109.
[8] Pinarbasi, A., and Ozalp, C., 2001, "Effect of Viscosity Models on the Stability of a Non-Newtonian Fluid in a Channel With Heat Transfer," Int. Commun. Heat Mass Transfer, **28**(3), pp. 369–378.
[9] Wazzan, A. R., Okamura, T. T., and Smith, A. M. O., 1968, "The Stability of Water Flow Over Heated and Cooled Flat Plates," Trans. ASME, Ser. C: J. Heat Transfer, **99**, pp. 109–114.
[10] Lauchle, G. C., and Gurney, G. B., 1984, "Laminar Boundary-Layer Transition on a Heated Underwater Body," J. Fluid Mech., **144**, pp. 79–101.
[11] Tritton, D. J., 1963, "Transition to Turbulence in the Free Convection Boundary Layers on an Inclined Heated Plate," J. Fluid Mech., **16**(3), pp. 417–435.
[12] Hu, J., Ben Hadid, H., Henry, D., and Mojtabi, A., 2008, "Linear Temporal and Spatio-Temporal Stability Analysis of a Binary Liquid Film Flowing Down an Inclined Uniformly Heated Plate," J. Fluid Mech., **599**, pp. 269–298.
[13] Herbert, D. M., 1963, "On the Stability of Visco-Elastic Liquids in Heated Plane Couette Flow," J. Fluid Mech., **17**(3), pp. 353–359.
[14] Strazisar, A. J., Reshotko, E., and Prahl, J. M., 1977, "Experimental Study of the Stability of Heated Laminar Boundary Layers in Water," J. Fluid Mech., **83**(2), pp. 225–247.
[15] Sukanek, P. C., Goldstein, C. A., and Laurence, R. L., 1973, "The Stability of Plane Channel Flow With Viscous Heating," J. Fluid Mech., **57**, pp. 651–670.
[16] Eldabe, N. T. M., El-Sabbagh, M. F., and El-Sayed(Hajjaj), M. A.-S., 2007, "The Stability of Plane Couette Flow of a Power-Law Fluid With Viscous Heating," Phys. Fluids, **19**, p. 094107.
[17] Yueh, C. S., and Weng, C. I., 1996, "Linear Stability Analysis of Plane Couette Flow With Viscous Heating," Phys. Fluids, **8**(7), pp. 1802–1813.
[18] Becker, L. E., and McKinley, G. H., 2000, "The Stability of Viscoelastic Creeping Plane Shear Flows With Viscous Heating," J. Non-Newtonian Fluid Mech., **92**, pp. 109–133.
[19] Ho, T. C., Denn, M. M., and Anshus, B. E., 1977, "Stability of Low Reynolds Number Flow With Viscous Heating," Rheol. Acta, **16**, pp. 61–68.
[20] Potter, M. C., and Graber, E., 1972, "Stability of Plane Poiseuille Flow With Heat Transfer," Phys. Fluids, **15**(3), pp. 387–391.
[21] Schäfer, P., and Herwig, H., 1993, "Stability of Plane Poiseuille Flow With Temperature Dependent Viscosity," Int. J. Heat Mass Transfer, **36**, pp. 2441–2448.
[22] Sameen, A., and Govindarajan, R., 2007, "The Effect of Wall Heating on Instability of Channel Flow," J. Fluid Mech., **577**, pp. 417–442.
[23] Wall, D. P., and Wilson, S. K., 1996, "The Linear Stability of Channel Flow of Fluid With Temperature Dependent Viscosity," J. Fluid Mech., **323**, pp. 107–132.
[24] Pinarbasi, A., and Liakopoulos, A., 1995, "Role of Variable Viscosity in the Stability of Channel Flow," Int. Commun. Heat Mass Transfer, **22**, pp. 837–847.
[25] Carrière, P., and Monkewitz, P., 1999, "Convective Versus Absolute Instability in Mixed Rayleigh–Benard–Poiseuille Convection," J. Fluid Mech., **384**, pp. 243–262.
[26] Yao, L. S., 1978, "Entry Flow in a Heated Straight Tube," J. Fluid Mech., **88**(3), pp. 465–483.
[27] Joseph, D. D., 1964, "Variable Viscosity Effects on the Flow and Stability of Flow in Channels and Pipes," Phys. Fluids, **7**, p. 1761.
[28] Davis, S. H., Kriegsmann, G. A., Laurence, R. L., and Rosenblat, S., 1983, "Multiple Solutions and Hysteresis in Steady Parallel Viscous Flows," Phys. Fluids, **26**(5), pp. 1177–1182.

[29] Pinarbasi, A., and Imal, M., 2005, "Viscous Heating Effects on the Linear Stability of Poiseuille Flow of an Inelastic Fluid," J. Non-Newtonian Fluid Mech., **127**, pp. 67–71.
[30] Thomas, D. G., Sureshkumar, R., and Khomami, B., 2004, "Thermo-Mechanical Instabilities in Dean and Taylor–Couette Flows: Mechanisms and Scaling Laws," J. Fluid Mech., **517**, pp. 251–279.
[31] Thomas, D. G., Sureshkumar, R., and Khomami, B., 2003, "Influence of Fluid Thermal Sensitivity on the Thermo-Mechanical Stability of the Taylor–Couette Flow," Phys. Fluids, **15**(11), pp. 3308–3317.
[32] Al-Mubaiyedh, U. A., Sureshkumar, R., and Khomami, B., 1999, "Influence of Energetics on the Stability of Viscoelastic Taylor–Couette Flow," Phys. Fluids, **11**(11), pp. 3217–3226.
[33] Al-Mubaiyedh, U. A., Sureshkumar, R., and Khomami, B., 2002, "The Effect of Viscous Heating on the Stability of Taylor–Couette Flow," J. Fluid Mech., **462**, pp. 111–132.
[34] White, J. M., and Muller, S. J., 2002, "Experimental Studies on the Stability of Newtonian Taylor–Couette Flow in the Presence of Viscous Heating," J. Fluid Mech., **462**, pp. 133–159.
[35] White, J., and Muller, S., 2000, "Viscous Heating and the Stability of Newtonian and Viscoelastic Taylor–Couette Flows," Phys. Rev. Lett., **84**, pp. 5130–5133.
[36] Nahme, R., 1940, "Beiträge zur hydrodynamischen theorie der lagerreibung," Ing. -Arch., **11**, pp. 191–209.
[37] Rayleigh, L., 1879, "On the Stability of Certain Fluid Motions," Proc. London Math. Soc., **s1–11**, pp. 57–72.
[38] Govindarajan, R., L'vov, V. S., and Procaccia, I., 2001, "Retardation of the Onset of Turbulence by Minor Viscosity Contrasts," Phys. Rev. Lett., **87**, p. 174501.
[39] Sahu, K. C., Valluri, P., Spelt, P. D. M., and Matar, O. K., 2007, "Linear Instability of Pressure-Driven Channel Flow of a Newtonian and Herschel–Bulkley Fluid," Phys. Fluids, **19**, p. 122101.
[40] Sahu, K. C., and Govindarajan, R., 2005, "Stability of Flow Through a Slowly Diverging Pipe," J. Fluid Mech., **531**, pp. 325–334.
[41] Orszag, S. A., 1983, "Accurate Solution of the Orr–Sommerfeld Stability Equation," J. Fluid Mech., **128**, pp. 347–385.
[42] Boomkamp, P. A. M., and Miesen, R. H. M., 1996, "Classification of Instabilities in Parallel Two-Phase Flow," Int. J. Multiphase Flow, **22**, pp. 67–88.
[43] Sahu, K. C., Ding, H., Valluri, P., and Matar, O. K., 2009, "Linear Stability Analysis and Numerical Simulation of Miscible Channel Flows," Phys. Fluids, **21**, p. 042104.
[44] Selvam, B., Merk, S., Govindarajan, R., and Meiburg, E., 2007, "Stability of Miscible Core—Annular Flows With Viscosity Stratification," J. Fluid Mech., **592**, pp. 23–49.